Design of a Stereo Handheld Camera Tool for Single Port Laparoscopy

Kai Xu[1], Zhengchen Dai[1], Bo Feng[2], and Jiangran Zhao[1]

[1] RII Lab (Lab of Robotics Innovation and Intervention), UM-SJTU Joint Institute,
[2] The Affiliated Ruijin Hospital,
Shanghai Jiao Tong University, Shanghai, 200240, China
{k.xu,zhengchen.dai,zjr318}@sjtu.edu.cn, fengbo2022@163.com,

Abstract. SPL (Single Port Laparoscopy) might bring improved surgical outcomes but this new procedure needs effective and functional next-generation surgical tools. Although several robotic systems for SPL have been constructed, only manual SPL tools are currently used in clinical SPL procedures. This paper presents the design, construction and experimental characterizations of a stereo handheld camera tool with integrated illumination for SPL. The camera tool can be folded for the insertion into abdomen through a Ø12mm trocar. Besides providing 3D visualization and illumination of the surgical scene, it can also be unfolded to spare an additional access port for other surgical tools. The actual effectiveness of this camera tool could be further gauged in a surgical setting with other manual SPL tools.

Keywords: Single Port Laparoscopy, handheld tool, stereo camera tool.

1 Introduction

SPL (Single Port Laparoscopy) uses one skin incision (e.g., the umbilicus) for laparoscopic interventions [1]. Compared with traditional multi-port laparoscopy, SPL could bring better surgical outcomes, including lower complication rates, less postoperative pain, shorter hospitalization and better cosmesis under a similar setting [2]. Although the newly introduced NOTES (Natural Orifice Translumenal Endoscopic Surgery) procedures [3] might lead to less invasiveness, NOTES is still quite far away from large scale clinical trials, even assisted by the special tools [4] or the robotic systems [5-11].

Using the newly developed SPL instruments, including the TriPort (Advanced Surgical Concepts), the SILS port (Covidien), the RealHand tools (Novare Surgical Systems), the Cambridge Endo instruments, etc., surgeons have found SPL a viable choice over traditional multi-port laparoscopy [12].

Although robotic systems for SPL [13-17] could be used to ease the difficult hand-eye coordination, these robotic systems are often associated with regulatory hurdles and high costs. Manual SPL tools are cheaper and could prevail more easily even though surgeons need to go through additional trainings.

X. Zhang et al. (Eds.): ICIRA 2014, Part II, LNAI 8918, pp. 299–310, 2014.

This paper hence presents the design of a stereo handheld camera tool with integrated illumination for SPL, as shown in Fig 1. While folded, the tool has a cylindrical laparoscope form with an outer diameter of 12mm. This form facilitates its insertion into abdomen through a Ø12mm trocar. The camera tool can then be unfolded to spare an access port as well as provide 3D visualization and illumination of the surgical scene. Other manual SPL tools could be deployed through this additional access port.

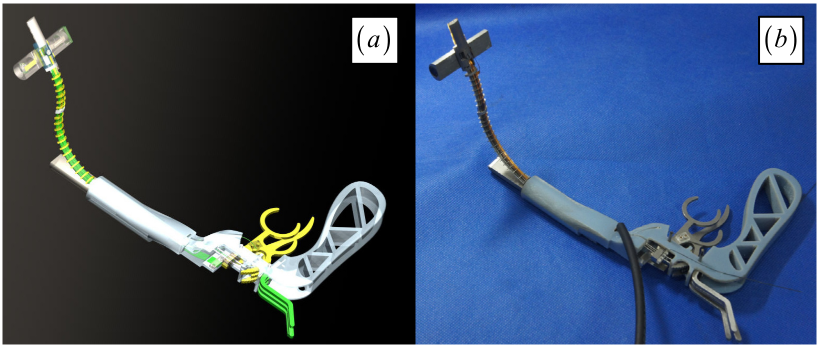

Fig. 1. The stereo handheld camera tool for SPL: (a) CAD model, and (b) prototype

Main contributions of this paper include i) the foldable structure of the camera tool which spares an additional access port for other instruments, ii) the incorporation of a continuum arm for camera head positioning, and iii) the use of mirrors in the camera head which allows the installation of two Ø7.8mm camera chips inside the Ø12mm camera head.

The paper is organized as follows. Section 2 presents the design goals and the overview. Detailed descriptions of the camera tool are presented in Section 3. Section 4 reports the experimental characterization of the camera tool with the conclusions followed in Section 5.

2 Design Goals and Overview

Attempting to address the increasing needs for SPL tools, this paper proposes the design of a foldable stereo handheld camera tool.

When the camera tool is in its folded configuration, the distal part of the tool possesses a Ø12mm cylindrical form so that it can be easily inserted into abdomen through a skin incision (e.g., the umbilicus). After insertion, the camera tool can then be unfolded to spare an additional access port as well as provide 3D visualization and illumination of the surgical scene.

A proposed use of the stereo camera tool could be seen from Fig. 2. The camera tool has unfolded itself and the access port spared inside the camera tool is big enough to pass a standard laparoscopic tool (e.g. the Ø5mm Harmonic scalpel from Ethicon Inc. or other Ø5mm tools). The access port could also be used for water or gas. Two needle-like laparoscopic instruments (e.g. the MiniLap tools from Stryker or the Mini-Laparoscopy tools from Karl Storz) can be inserted into the patient's abdomen for tissue manipulations.

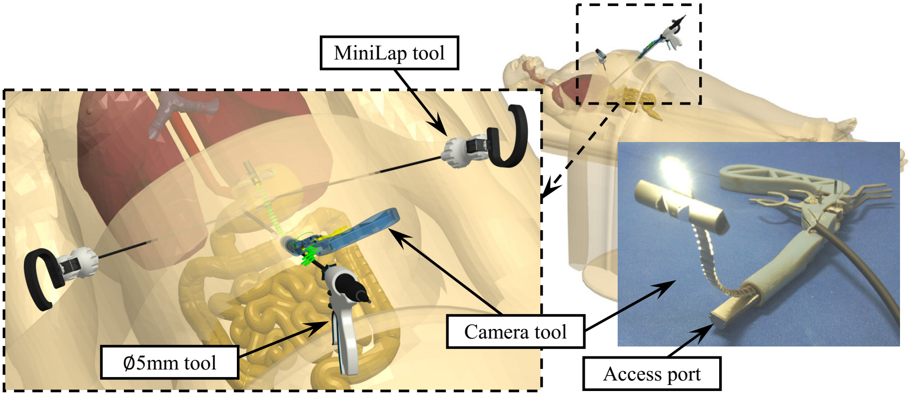

Fig. 2. The proposed use of the handheld camera tool

Considering the intended application of this camera tool, the conceived CAD model and the constructed prototype are shown in Fig. 1. The design's features can be highlighted as follows.

- The distal part of the camera tool only possesses an outer diameter of 12mm in its folded configuration. This is inspired by the Ø12mm endoscopic robot as in [9, 11].
- The use of mirrors allows the installation of two Ø7.8mm camera chips inside the Ø12mm camera head. Relatively big camera chips could bring better image qualities.
- An imaging distance of 100mm to 150mm from the access port to the objects is achieved.
- A 3-DoF continuum arm is incorporated to orient and position the camera head in order to achieve dexterous viewing perspectives of the surgical site.
- Illumination using LEDs are integrated.

Section 3 presents the detailed components descriptions, including the arrangement of the camera chips, the design of a pivoting mechanism, dimension determination of the continuum arm, and the design of the tool handle. Experimental characterizations are reported in Section 4.

3 Components Descriptions

Design of the handheld camera tool include i) the camera head with two camera chips, ii) the pivoting mechanism for the camera head, iii) the continuum arm, iv) the illumination design, and v) the design of the tool handle. These components are described here with sufficient details.

3.1 Design of the Camera Head

It's desired to use high quality camera chips for the camera head. Usually bigger camera chips have better imaging qualities. Among the available products from several major suppliers of miniature camera chips, MO-B3506 (MISUMI Electronics Corp, 640×480 resolution, 50dB S/N ratio, and 0.1 Lux minimal illuminations) is selected, as shown in the inset of Fig. 3. The camera chips at smaller sizes can't provide imaging qualities that are good enough.

In order to fit the two Ø7.8mm MO-B3506 camera chips inside the Ø12mm camera head for stereo visualization, an axial arrangement of the two camera chips were used. As shown in Fig. 3(a), two mirrors are used to reflect the images. The axially arranged camera chips now have equivalent radial orientations because of the mirrors. The distance between the two mirror centers is 11mm and the distance between the two camera chips is 20mm. If γ_1 (the angle between the two mirrors) is equal to 90°, the two equivalent camera chips have parallel axes. By adjusting γ_1, γ_2 (the angle between the two equivalent camera chip axes) can be varied as in Eq. (1).

$$\gamma_2 = 2\gamma_1 - 180^\circ \quad . \tag{1}$$

A series of experiments were conducted to adjust the γ_1 angle for better 3D perception for human, as shown in Fig. 4(c). The anaglyph views were shown to several human subjects and they picked one that looked the most natural. The γ_1 angle was then chosen to be 92°.

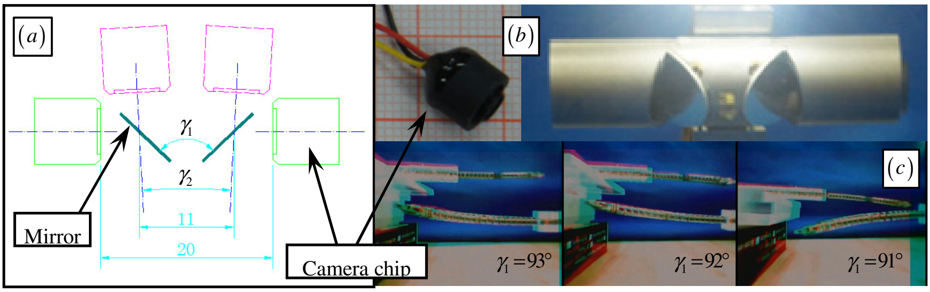

Fig. 3. Camera chip arrangement in the camera head: (a) the schematic, (b) the prototype, and (c) experiments to adjust the camera chip axes

3.2 A Pivoting Mechanism for the Camera Head

The mirrors in the camera head are axially arranged. The camera head has to be rotated for 90°, in order to generate a normal stereo view. A pivoting mechanism is designed as in Fig. 4 to rotate the camera head about the pivoting screw to transform the distal part of the tool from the cylindrical form into the unfolded configuration.

As shown in Fig. 4(a), the actuation block can be pushed and pulled by the actuation rod to move along the pin guide. Outer shape of the actuation block is fabricated to make sure that the camera head is entirely within the Ø12mm cylindrical shape when the camera head is folded. The actuation rod is a Ø0.4mm super-elastic nitinol. When the actuation block is driven, it pushes a driving pin to rotate the camera head between 0° and 90°, as shown in Fig. 4(b).

FlexPCB strips were used to replace the camera chips' original wires so that the wires will not get tangled during the rotating motions of the camera head. As shown in Fig. 4(c), the FlexPCB strips were carefully patterned and arranged inside the camera head so that the rotation of the camera head is not affected by the FlexPCB strips.

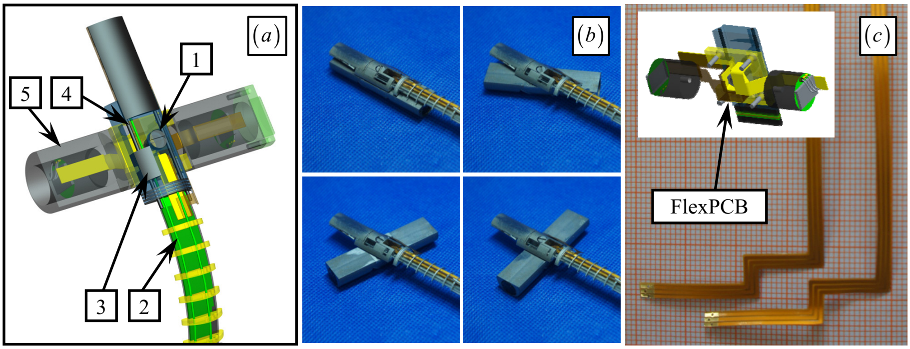

Fig. 4. The pivoting mechanism for the camera head: (a.1) pivoting screw, (a.2) actuation rod, (a.3) actuation block, (a.4) pin guide, (a.5) camera head, (b) the motion sequence, and (c) arrangement of the FlexPCB

3.3 Design of the Continuum Arm

A continuum arm is incorporated so that the camera head can be better positioned and oriented when the handle is constrained by the inserted extra tool though the access port. As shown in Fig. 5, the continuum arm consists of i) actuation rods, ii) a super-elastic nitinol strip, iii) a fixation ring, and iv) several spacers.

The fixation ring is attached at the middle of the nitinol strip. The nitinol strip between the fixation ring and the arm entrance is referred to as segment #1. The nitinol strip between the camera head and the segment #1 is referred to as segment #2.

Two actuation rods are connected to the fixation ring and can slide in the spacers' holes. Pulling of the actuation rod would bend the segment #1 upwards. Another actuation rod is connected to the camera head and can slide in the spacers. Pushing this actuation rod would bend the segment #2 downwards.

The third DoF (Degree of Freedom) of the continuum arm is the translational feed of the segment #1.

Bending shapes of the segments #1 and #2 are assumed to be circular according to the previous studies as in [18, 19]. Using this assumption, some derivations could be carried out to calculate the segments' desired lengths.

The preferred viewing distance of the arm entrance (the access port) ranges from 100mm to 150mm. When the segment #1 is assumed for a 90º bending, the following can be derived.

$$\begin{cases} \overline{OC} = \dfrac{2L_1}{\pi} + \dfrac{L_2}{\vartheta}(1-\cos\vartheta) \\ \overline{BC} = \dfrac{2L_1}{\pi} + \dfrac{L_2}{\vartheta}\sin\vartheta \\ \overline{CD} = \dfrac{\overline{BC}}{\tan\vartheta} = \dfrac{2L_1}{\pi}\dfrac{\cos\vartheta}{\sin\vartheta} + \dfrac{L_2}{\vartheta}\cos\vartheta \end{cases} . \tag{2}$$

$$\overline{OD} = \overline{OC} + \overline{CD} = \frac{2L_1}{\pi}\left(1+\frac{\cos\vartheta}{\sin\vartheta}\right) + \frac{L_2}{\vartheta} . \tag{3}$$

If the segment #2 bends from 0º to 90º, it is preferred for the viewing direction to point towards the middle of the viewing range when $\vartheta = 45°$. Then Eq. (3) gives:

$$\overline{OD} = \frac{4}{\pi}(L_1 + L_2) \rightarrow 125mm . \tag{4}$$

Many L_1 and L_2 values satisfy Eq. (4). $L_1 = 60mm$ and $L_2 = 40mm$ are used.

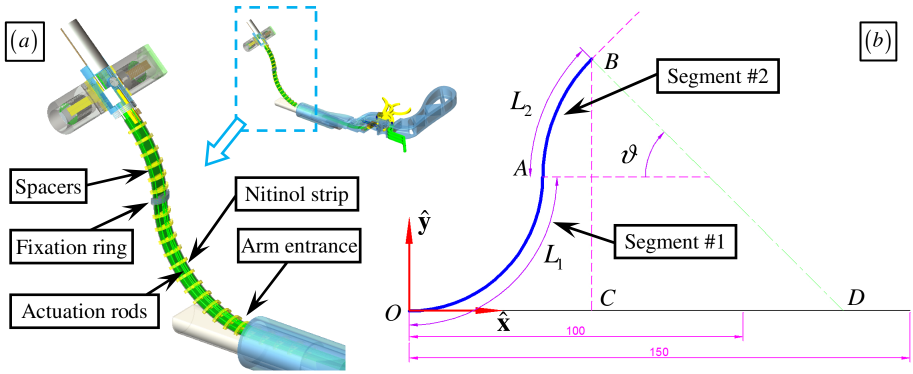

Fig. 5. The continuum arm: (a) structure and (b) dimension calculation

3.4 Onboard LEDs for Illumination

Six LEDs were planned for the illumination of surgical scenes as shown in Fig. 6(a). A FlexiPCB strip was used to mount and power the LEDs as in Fig. 6(d).

Temperature rise could be a concern while using LEDs for illumination. A series of experiments were carried out to investigate the potential heating problem. The LEDs were powered at different voltages in an indoor environment and temperatures of the LEDs were measured.

The LED has a rated voltage of 2.95v. It was found that powering the LEDs at this voltage will always cause heating problems. Then it was decided to power the LEDs at 2.70v, since no heating problems were identified under this voltage.

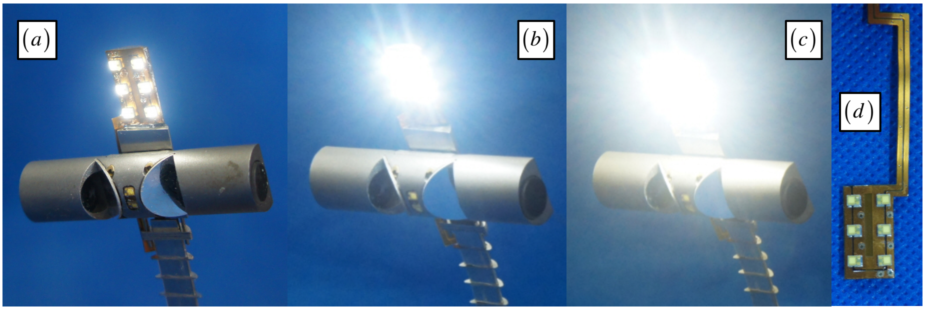

Fig. 6. Illumination tests with LEDs powered at (a) 2.50v, (b) 2.60v and (c) 2.70v; (d) FlexPCB

3.5 Design of the Handle

The handle is used to hold and manipulate this camera tool. In order to avoid interferences when an additional surgical tool is inserted through the access port, the handle is designed to be horizontally placed as shown in Fig.2 and Fig. 11.

The camera head of the designed handheld tool needs three actuation inputs: i) two inputs for the bending of the segments #1 and #2 of the continuum arm, and ii) one input for the pivoting mechanism.

The three inputs are realized by the triggers #1 ~ #3 as shown in Fig. 7. The trigger #1 actuates two actuation rods of the segment #1; the trigger #2 actuates the actuation rod of the segment #2 by pushing the driving pin which is guided by the actuation slider; and the trigger #3 actuates the actuation rod of the pivoting mechanism. These actuation rods are routed inside the channels in the handle that was fabricated using 3D printing.

All the three triggers have a ratchet-like feature so that the actuation rods could be locked in position. The tooth profiles on the triggers are carefully designed such that the actuation rods will be pushed or pulled approximately 1mm per tooth. Three spring-loaded releases (#1 to #3) could be pressed by a user's thumb to release these triggers and allow the actuation rods to be released.

The use of the handle is explained in Section 4.1.

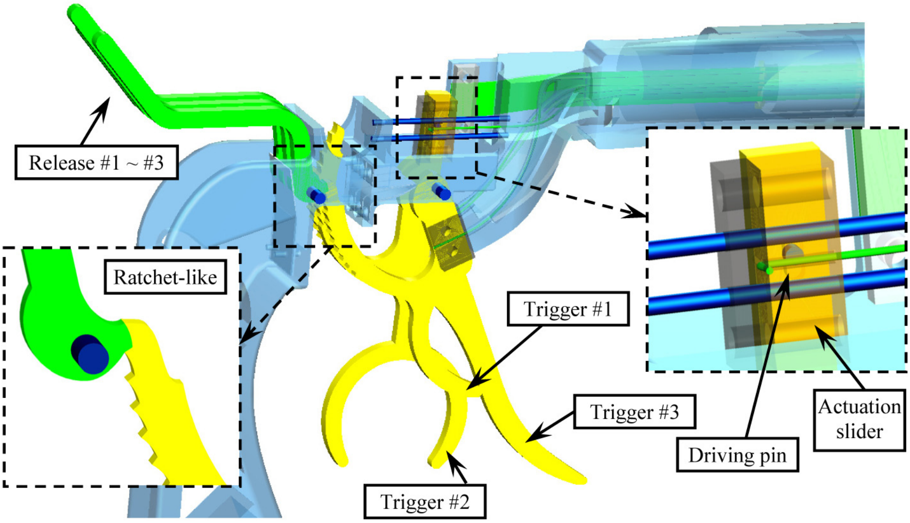

Fig. 7. Design of the tool handle

4 Ex-Vivo Experimental Characterization

After the handheld camera tool is fabricated and assembled, several experiments were conducted to characterize the features of this tool.

4.1 Tool Deployment

The handheld camera tool shall be inserted into abdomen in its folded form as shown in Fig. 8(a). The distal part of the tool has a cylindrical outer shape. The tool could be actuated to unfold itself using the three triggers and then provide illumination and 3D visualization of surgical scenes. This deployment is as follows.

After insertion into abdomen, the handle can further extend the continuum arm through the tube, as shown in Fig. 8(b). Then the trigger #1 can be pulled to bend the segment #1 of the continuum arm upwards. And the trigger #2 can be pushed to bend the segment #2 of the arm downwards. The trigger #3 can be pulled to rotate the camera head to provide a horizontal stereo view of the surgical site. The rotation motion of the camera head could also be seen from Fig. 4(b). The camera tool is then fully deployed as shown in Fig. 8(c).

The LEDs would be powered on to provide illumination. The triggers and the releases can be used together to adjust the continuum arm to a desired pose.

Other surgical tools can be later deployed through the access port spared within this handheld tool. Since the direction of the access port could be constrained by the newly inserted tool, the continuum arm allows dexterous positioning and orienting of the camera head by adjusting the triggers and the releases.

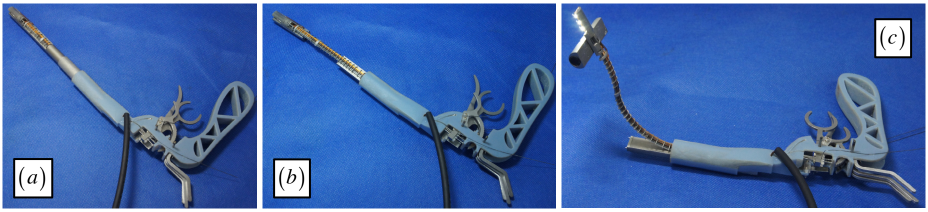

Fig. 8. Tool deployment

4.2 Shape Identification of the Continuum Arm

The dimensions of the continuum arm were calculated in Section 3.3 based on an assumption that both the segment #1 and the segment #2 have circular bending shapes. The experiments reported here were conducted to verify this assumption.

The experimental setup is shown in Fig. 9(a). An optical tracker (Micron Tracker SX60 from Claron Technology Inc.) was used with a pointer. The pointer was pointed at different positions along the continuum arm. The tracker could directly provide the coordinates of the pointer's tip.

The coordinates of the points along the continuum arm were recorded, transformed to $\{\hat{\mathbf{x}}, \hat{\mathbf{y}}\}$ as defined in Fig. 5, and plotted in Fig. 9(b). Two serially connected circular arcs approximate the bent segment #1 and the bent segment #2, whereas a circular arc with a straight line segment approximates the bent segment #1 and the straight segment #2.

The experimental results clearly indicate that the actual shapes of the segments can be well approximated by circular arcs.

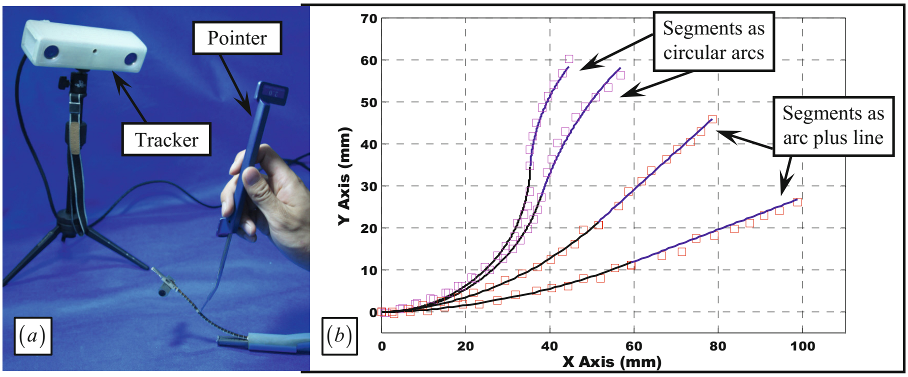

Fig. 9. Shape identification of the tool's continuum arm

4.3 Calibration of the Camera Chips

In order to improve the imaging quality, the camera chips might be calibrated.

The calibration was implemented using the Camera Calibration Toolbox for Matlab. The toolbox uses existing algorithms [20]. As shown in Fig. 10(a), several photos were taken for a calibration board. The corners were repeatedly detected to obtain the distortion correction coefficients. The distortion can be visualized as shown in Fig. 10(b). The calibration was conducted for both camera chips. The parameters were obtained, including the focal lengths, the principal points, the skew coefficient, the distortion coefficients, etc.

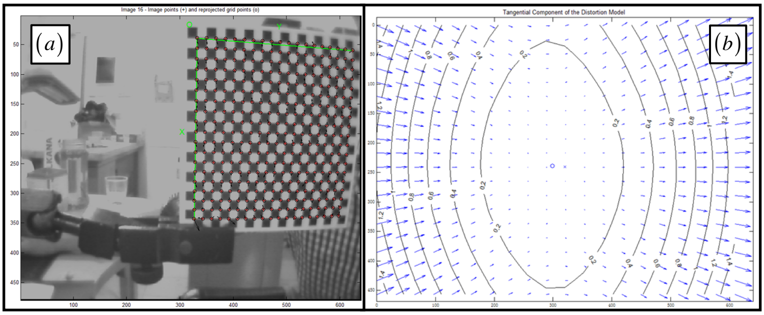

Fig. 10. Camera chip calibration: (a) calibration board, and (b) distortion visualization

4.4 Ex-vivo Trial of the Handheld Camera Tool

The camera tool was also tested in an ex-vivo trial. As in Fig. 11(a), an abdomen under pneumoperitoneum was mimicked by a box. The camera tool was deployed and another tool was inserted. The scene was visualized with illumination provided by the LEDs. The anaglyph view assembled from both camera chips is shown in Fig. 11(b).

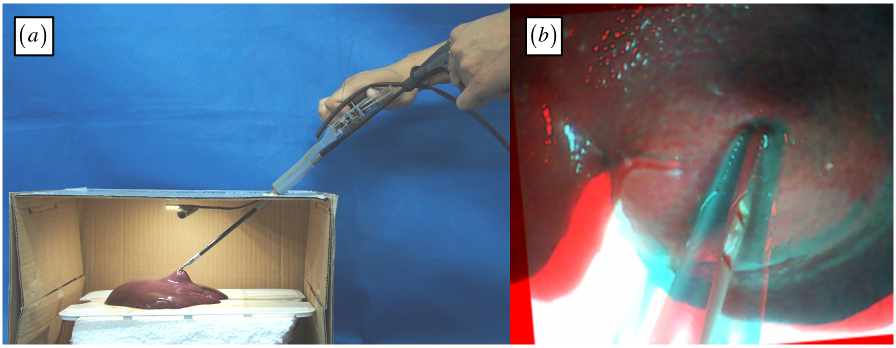

Fig. 11. Ex-vivo trial of the camera tool: (a) setup, (b) anaglyph view

5 Conclusions and Future Work

This paper presents the design, construction, and experimental characterizations of a stereo handheld camera tool with onboard illumination for SPL.

The distal part of the camera tool can be folded into a Ø12mm cylindrical form for the insertion into abdomen. Then it can be actuated to unfold itself using three triggers, providing illumination and 3D visualization of surgical scenes. An additional access port can also be spared inside the tool to insert other surgical tools.

Several sets of experiments were conducted to demonstrate the functionality and characteristics of this handheld camera tool. Particularly, the camera tool successfully visualized a mockup surgical scene using its integrated LEDs. An anaglyph view was generated and another surgical tool was inserted through the spared access port to perform tissue manipulations.

The future work shall focus on improving the reliability and sterilizability of this design so that the tool can be truly gauged in a more realistic setting.

Acknowledgments. This work was supported in part by the National Natural Science Foundation of China (Grant No. 51375295), in part by the Shanghai Rising-Star Program (Grant No. 14QA1402100), and in part by the Shanghai Jiao Tong University Interdisciplinary Research Funds (Grant No. YG2013MS26).

References

1. Navarra, G., Pozza, E., Occhionorelli, S., Carcoforo, P., Donini, I.: One-Wound Laparoscopic Cholecystectomy. British Journal of Surgery 84(5), 695 (1997)
2. Podolsky, E.R., John-Dillon, L., King, S.A., Curcillo II, P.G.: Reduced Port Surgery: An Economical, Ecological, Educational, and Efficient Approach to Development of Single Port Access Surgery. Surgical Technology International (20), 41–46 (2010)
3. Kalloo, A.N., Singh, V.K., Jagannath, S.B., Niiyama, H., Hill, S.L., Vaughn, C.A., Magee, C.A., Kantsevoy, S.V.: Flexible Transgastric Peritoneoscopy: A Novel Approach to Diagnostic and Therapeutic Interventions in the Peritoneal Cavity. Gastrointestinal Endoscopy 60(1), 114–117 (2004)
4. Hu, B., Chung, S., Sun, L.C.L., Kawashima, K., Yamamoto, T., Cotton, P.B., Gostout, C.J., Hawes, R.H., Kalloo, A.N., Kantsevoy, S.V., Pasricha, P.J.: Eagle Claw II: A Novel Endosuture Device that Uses a Curved Needle for Major Arterial Bleeding: A Bench Study. Gastrointestinal Endoscopy 62(2), 266–270 (2005)
5. Abbott, D.J., Becke, C., Rothstein, R.I., Peine, W.J.: Design of an Endoluminal NOTES Robotic System. In: IEEE/RSJ International Conference on Intelligent Robots and Systems (IROS), San Diego, CA, USA, pp. 410–416 (2007)
6. Phee, S.J., Low, S.C., Sun, Z.L., Ho, K.Y., Huang, W.M., Thant, Z.M.: Robotic System for No-Scar Gastrointestinal Surgery. The International Journal of Medical Robotics and Computer Assisted Surgery 4(1), 15–22 (2008)
7. Lehman, A.C., Dumpert, J., Wood, N.A., Redden, L., Visty, A.Q., Farritor, S., Varnell, B., Oleynikov, D.: Natural Orifice Cholecystectomy using a Miniature Robot. Surgical Endoscopy 23(2), 260–266 (2009)

8. Xu, K., Zhao, J., Geiger, J., Shih, A.J., Zheng, M.: Design of an Endoscopic Stitching Device for Surgical Obesity Treatment Using a N.O.T.E.S Approach. In: IEEE/RSJ International Conference on Intelligent Robots and Systems (IROS), San Francisco, CA, USA, pp. 961–966 (2011)
9. Xu, K., Zhao, J., Shih, A.J.: Development of an Endoscopic Continuum Robot to Enable Transgastric Surgical Obesity Treatment. In: Su, C.-Y., Rakheja, S., Liu, H. (eds.) ICIRA 2012, Part I. LNCS (LNAI), vol. 7506, pp. 589–600. Springer, Heidelberg (2012)
10. Tortora, G., Salerno, M., Ranzani, T., Tognarelli, S., Dario, P., Menciassi, A.: A Modular Magnetic Platform for Natural Orifice Transluminal Endoscopic Surgery. In: Annual International Conference of the IEEE Engineering in Medicine and Biology Society (EMBC), Osaka, Japan, pp. 6265–6268 (2013)
11. Zhao, J., Zheng, X., Zheng, M., Shih, A.J., Xu, K.: An Endoscopic Continuum Testbed for Finalizing System Characteristics of a Surgical Robot for NOTES Procedures. In: IEEE/ASME International Conference on Advanced Intelligent Mechatronics (AIM), Wollongong, Australia, pp. 63–70 (2013)
12. Rao, P.P., Rao, P.P., Bhagwat, S.: Single-incision Laparoscopic Surgery - Current Status and Controversies. Journal of Minimal Access Surgery 7(1), 6–16 (2011)
13. Piccigallo, M., Scarfogliero, U., Quaglia, C., Petroni, G., Valdastri, P., Menciassi, A., Dario, P.: Design of a Novel Bimanual Robotic System for Single-Port Laparoscopy. IEEE/ASME Transactions on Mechatronics 15(6), 871–878 (2010)
14. Sekiguchi, Y., Kobayashi, Y., Tomono, Y., Watanabe, H., Toyoda, K., Konishi, K., Tomikawa, M., Ieiri, S., Tanoue, K., Hashizume, M., Fujie, M.G.: Development of a Tool Manipulator Driven by a Flexible Shaft for Single Port Endoscopic Surgery. In: IEEE / RAS-EMBS International Conference on Biomedical Robotics and Biomechatronics (BIOROB), Tokyo, Japan, pp. 120–125 (2010)
15. Lee, H., Choi, Y., Yi, B.-J.: Stackable 4-BAR Manipulators for Single Port Access Surgery. IEEE/ASME Transaction on Mechatronics 17(1), 157–166 (2012)
16. Xu, K., Goldman, R.E., Ding, J., Allen, P.K., Fowler, D.L., Simaan, N.: System Design of an Insertable Robotic Effector Platform for Single Port Access (SPA) Surgery. In: IEEE/RSJ International Conference on Intelligent Robots and Systems (IROS), St. Louis, MO, USA, pp. 5546–5552 (2009)
17. Ding, J., Goldman, R.E., Xu, K., Allen, P.K., Fowler, D.L., Simaan, N.: Design and Coordination Kinematics of an Insertable Robotic Effectors Platform for Single-Port Access Surgery. IEEE/ASME Transactions on Mechatronics 18(5), 1612–1624 (2013)
18. Xu, K., Simaan, N.: Analytic Formulation for the Kinematics, Statics and Shape Restoration of Multibackbone Continuum Robots via Elliptic Integrals. Journal of Mechanisms and Robotics 2(011006), 1–13 (2010)
19. Webster, R.J., Jones, B.A.: Design and Kinematic Modeling of Constant Curvature Continuum Robots: A Review. International Journal of Robotics Research 29(13), 1661–1683 (2010)
20. Zhang, Z.: Flexible Camera Calibration by Viewing a Plane from Unknown Orientations. In: IEEE International Conference on Computer Vision (ICCV), Kerkyra, pp. 666–673 (1999)